EXPERIMENTAL CHARACTERISATION OF DOMINANT DRIVING FORCES AND FLUCTUATING VENTILATION RATES FOR A SINGLE SIDED SLOT LOUVER VENTILATION SYSTEM

Paul D O'Sullivan[1, 2], Maria Kolokotroni [2]

1. *School of Mechanical, Electrical & Process Engineering, Cork Institute of Technology, Cork, Rossa Avenue, Bishopstown, Cork, Ireland*
2. *Howell Building, Mechanical Engineering, School of Engineering and Design, Brunel University, Uxbridge UB8 3PH, United Kingdom*

ABSTRACT

Adopting natural ventilation as a retrofit strategy for cooling, due to the low impact nature of the installation, is attractive due to the cooling potential of untreated outdoor air for large periods of the extended cooling season, particularly in northern climates. In line with this it is important to characterise the performance of natural ventilation components in low energy buildings in successfully transferring the cooling potential of outdoor air to the occupied zone. This paper presents an analysis of the results from 25 individual ventilation rate tests of a single sided slot louver ventilation system installed in a low energy retrofit application and 13 tests from a pre-retrofit window opening, taken as a control space for comparative purposes. Results for 3 opening configurations for the slot louver ventilation system are compared. Parameters characterising momentum and buoyancy driving forces during each test were also recorded. A number of different permutations for combined wind and buoyancy effects were recorded allowing an investigation of the existence of any underlying patterns as well as the relative effect of the different opening configurations. Owing to the nature of single sided ventilation and the primary airflow exchange mechanisms normally present, the transient evolution of the normalised tracer gas concentration during tests is also discussed and compared. Analysis shows that different patterns emerge for the dominant driving forces depending on opening configuration in the slot louver system. The slot louver ventilation system has led to steadier ventilation rates. Opening height and geometry is shown to have a significant effect on the net contribution from momentum driving forces and the fluctuation amplitude of the ventilation rate and this effect is wind direction dependant. Ventilation rates are shown to correlate well with fluctuation amplitude. The nature of the ventilation rate during tests for different wind directions is shown to vary depending on wind patterns at the building envelope.

KEYWORDS

Single sided ventilation, dominant forces, warren plot, buoyancy asymptote, fluctuating ventilation rate

1 INTRODUCTION

While experimental data exists for single sided ventilation rates, (Dascalaki et al 1996) (Dascalaki et al. 1995) (de Gids and Pfaff. 1982) (Caciolo et al 2011), information is not exhaustive for opening types other than common window types. Single sided ventilation techniques are generally reserved for single cell (Irving et al 2005), isolated spaces and when considering older office buildings that need retrofitting, the floor plan can often be cubicle and not intended as open plan spaces. Developing ventilation components that can be externally applied, provide sufficient weather protection and are effective at ensuring good ventilation rates by responding to contributing airflow mechanisms is central to ensuring successful implementation of climate change adaptation strategies. This paper presents an analysis of the mechanisms contributing to time average single sided ventilation rates from test results for a slot louvre ventilation component operated as part of a single sided ventilation strategy. It considers two key aspects of the ventilation rate; the combined effect of momentum and buoyancy forces on mean ventilation rates and analysis of the nature of the ventilation rate during tracer decay tests using a fluctuation parameter, σ_c. The objective is to

Nomenclature

Symbols		*Subscripts*	
Ar	Archimedes Number	i	inside
F	Flow Number	o	outside
K	constant related to C_d for opening	ie	internal to external
C_d	discharge coefficient	ACH	Air change rate
Re	Reynolds Number	t	Tracer, total
T	temperature (K)	th	Thermal, stack effect
H	height, (m)	ope	opening
g	gravitational constant, $(\mathrm{m/s^2})$	eff	effective
v	velocity, $(\mathrm{m/s})$	w	wind , test space envelope wall
q_{ACH}	time averaged air change rate, $(\mathrm{h^{-1}})$	N	Normalised concentration
A	opening area $(\mathrm{m^2})$	int	Zone interior
β	Power law exponent	h	hydraulic
L	Characteristic length (m)	c	concentration (relating to fluctuations)
ρ	Density $(\mathrm{kg/m^3})$		
C	tracer gas concentration (ppm)	*Abbreviations*	
t	time, (h)	CS	Control space
P	Total pressure ($\mathrm{kg/ms^2}$)	RS	Retrofit space
σ	standard error of estimate of predictions	ACH	Air change rate
		P	Parallel incidence direction
		L	Leeward incidence direction
		W	Windward incidence direction
		WD	Wind direction

investigate the conditions contributing to mean ventilation rates for a slot louvre system used in single sided ventilation. Data presented was recorded in a full scale test room for different opening configurations. Literature review has revealed little reported work of full scale experiments characterising how slot louvre systems with low hydraulic diameters perform within ventilation strategies where mechanisms such as turbulent eddy diffusion play an important function.

2 EXPERIMENTAL SETUP

A total of 25 full scale ventilation rate tests from the retrofit space for different component opening configurations were compared to 13 tests in a control space in the existing building with dynamically similar characteristics. Ventilation components tested are described in section 3. Experimental measurements were recorded using a tracer gas decay technique with the regression method applied to spatially averaged and normalised concentration values. All tests were completed under normal operating mode for the ventilation system resulting in the inclusion of effects from some complex geometry at the openings as well as a number of openings serving the test space being included in the recordings.. A detailed summary of the experimental setup and test conditions for both retrofit space and control space has recently been published by the authors and is not repeated here (O'Sullivan and Kolokotroni, 2014).

3 VENTILATION COMPONENT DETAILS

3.1 Slot louvre ventilation system (RS.02, RS.03, RS.04)

The installed slot louvre system has a net 50% free open area for airflow and overall structural opening dimensions are 0.30m (w) x 1.60m (h) with a net opening area of 0.102 $\mathrm{m^2}$ (2 openings at low level and 2 openings at high level in the test space). On the internal side of the slot louvres there are automated higher level insulated doors and manual lower level insulated doors providing different control mechanisms. The ventilation system forms part of an externally applied retrofit fenestration module supplied with two glazed sections and two ventilation sections. The louvres are manufactured in anodized aluminium alloy 6063-T6 with a resulting smooth surface finish, see Figure 1. Each of the ventilation openings has 17 airflow slots across the louvre bank. Taken individually the louvre slots have an extremely low porosity at 0.057%. Table 1 summarises key information regarding the slot louvre system.

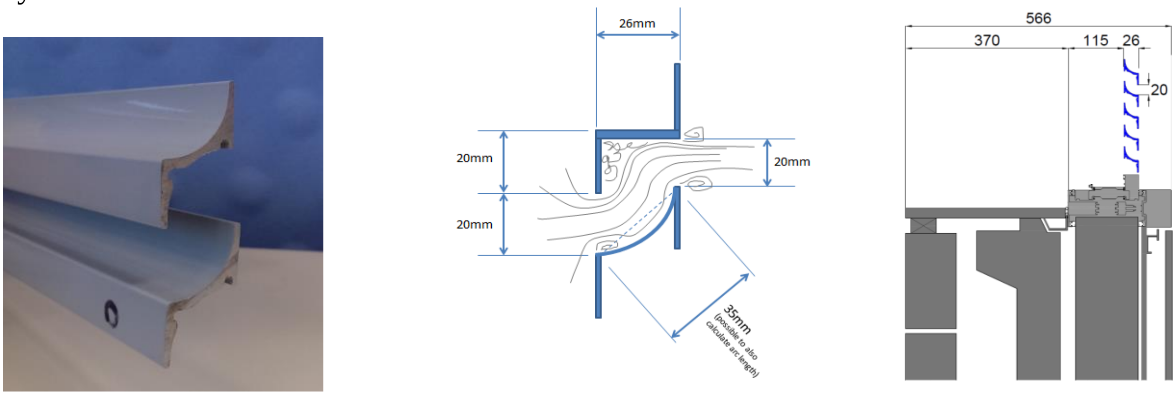

Figure 1: Slot louvre component details (a) sample louvre profile, (b) opening dimensions (c) installation

3.2 Top hung outward opening window (CS.01)

The control space ventilation component consists of an outward opening top hung window unit. This was used as a basis for comparison of time average ventilation rates and ventilation unsteadiness during tests with the slot louvre system. Details are summarised in Table 1 and in (O'Sullivan and Kolokotroni. 2014). There appears to be limited data available on full scale performance of this type of window in the literature. Recently Grabe has done some work characterising flow resistance (Grabe 2013).

Table 1: comparison of purpose provided ventilation opening types in CS & RS

Parameter	CS	RS	Units
Plain structural opening dimensions (W x H)	0.92 x 1.14	0.30 x 1.60	m
Total opening area A_t	0.32	0.42	m^2
Porosity	0.18	0.057	(%)
Total opening "wetted" perimeter	5.96	0.99	m
Hydraulic diameter (d_h) (A_t & based on "wetted" perimeter)	0.214	0.02	m
Aspect Ratio (L/d_h)	1.070*	1.075	(-)
Opening type (categories according to Etheridge 2011)	short	short	(-)

*Note: length dimension for measured along perimeter of opening window section

3.3 Definition of F_{th} asymptote for ventilation components

Dimensional Analysis using Warren plots is predicated on the correct selection of the asymptote through the origin defining flow number due to buoyancy alone, F_{th}. The gradient of this asymptote is sensitive to correct selection of both the still air discharge coefficient, C_d and the exponent used in the power law relationship for pressure and flow (i.e. β = 0.5 for orifice flow). C_d is an important parameter for a ventilation opening as it depends on the geometry of the opening and the Reynolds number, R_e of the flow, and is normally taken as 0.61 for a flush faced sharp edged orifice. Various research studies have considered the effect on C_d of different opening types and their geometry, shape and porosity under wind driven flow (Karava et al 2004) (Heiselberg et al 2001), while other studies have concentrated on the effects of wind in terms of direction and the effects of dynamic pressure (Chiu and Etheridge 2007). Caciolo et al (Caciolo et al 2011) used a C_d value of 0.6 to describe the flow characteristic when calculating F_{th} for various open window geometries while a C_d of 1.0 is used in (Dascalaki et al 1996). Grabe has recently presented findings specific to flow conditions under buoyancy alone that relates to the definition of C_d for top hung outward opening windows (Grabe 2013; von Grabe et al 2014). The value selected for C_d for the control space window opening to facilitate analysis is 0.55 and is largely based on Grabe et al. Both Pinnock (Pinnock 2000) and Sharples et al (Sharples and Chilengwe 2006) have carried out experimental work considering the use of alternative exponent values in the power law equation when dealing with buoyancy alone case and slot louvres respectively. Pinnock proposed β = 0.6348 and Sharples suggested β = 0.9301. The orifice flow equation is retained for analysis here although this is something that warrants further investigation given the significant impact on $Ar^{\beta=0.5}$ this would have. The slot louvre system used here is a flush faced sharp edged orifice at the inlet and flow is likely unidirectional through the individual slot openings. There is a length component of the louvre in a circular shape (see Figure 1) that might promote some flow reattachment allowing viscous forces and a boundary layer to develop, reducing the flow separation that normally results in C_d being independent of Re. However, for the purposes of establishing a C_d value under buoyancy alone conditions 0.61 may be a little low but acceptable for RS.04 and RS.02 for the purposes of initial analysis. The RS.03 configuration has the combined effect of slot louvre and inward opening ventilation door due to its restricted opening angle and a C_d probably lower than 0.61 as a result. A C_d value of 0.55 is assumed for RS.03. Quantifying a correct C_d value and power law exponent for the slot louvre system is still under investigation and is not presented here.

4 CHARACTERISING DRIVING FORCES FOR SINGLE SIDED VENTILATION

The mechanisms that produce airflow in single sided ventilation are generated through varying combinations of wind and buoyancy forces acting at the opening. Depending on wind incidence angle the dominant mechanisms are either from a pulsating flow due to pressure difference at the opening, turbulent diffusion through a mixing layer at the opening plane or a combination of both. When due to buoyancy forces alone, the flow will be bidirectional with a neutral pressure at the opening mid height point. The temperature difference at the opening results in a buoyancy effect that produces a stable airflow exchange. However, at low wind speeds and a leeward incidence direction the effective enveloped temperature has been shown to be reduced due to a recirculation zone counteracting buoyancy effects resulting in air change rates lower than in the absence of wind (Caciolo et al 2013). When wind is normal to the opening plane a pulsation airflow effect will dominate increasing compression of the air mass but not necessarily adding to ventilation rate. Cockroft and Robertson suggested that 37% of the volume flowrate across the opening due to pulsation will contribute to an air change rate (Cockroft and Robertson. 1976). The local wind speed at the opening is very much dependant on wind direction due to changes in flow patterns along the envelope given different wind incidence directions. Larsen shows how air change rate depends on wind incidence direction with effect more pronounced at low wind speeds and the dominating force differs between wind speed and ΔT_{ie} depending on the ratio between these forces and the wind direction (Larsen and Heiselberg 2008). A number of semi empirical models exist that use Bernoulli flow theory and can also account for contributions from wind effects. Warren and Perkins (Warren and Parkins 1985) proposed 2 separate correlations for buoyancy and wind effect, taking the larger of the two to quantify ventilation rate. Dascalaki (Dascalaki et al 1996) proposed an alternative correlation to take account of wind effects. See also for example (Crommelin and Vrins. 1988), (De Gids and Pfaff. 1976), (Wang and Chen 2012). When studying permutations of contributing forces for ventilation rate tests Warren used the relationship between a dimensionless ventilation parameter, Flow Number F, and an adjusted Archimedes Number, $Ar^{0.5}$. The purpose of the Warren plot is to separate out the data dominated by buoyancy effect. Warren plots have been used by researchers to analyse air change rate data, for example see (Warren and Parkins 1985) (Van Der Mass. 1992), (Caciolo et al 2011). Archimedes Number, Ar, is used as a measure of the relative magnitudes of the buoyancy (gravity) forces and the momentum (inertial) forces acting on elements of fluid. This ratio can be expressed in (1) where L is a characteristic height.

$$\frac{gL\Delta\rho}{P_w} \tag{1}$$

For dynamically similar flows substituting ρv^2 for total wind pressure, P_w, and taking the square root one obtains a dimensionless parameter which is basically the same as that known as Ar (Etheridge, 2011):

$$Ar \equiv \sqrt{\frac{\Delta\rho g L}{\rho v^2}} \tag{2}$$

The ratio $\Delta\rho/\rho$ can be replaced with $\Delta T/T$ for cases of interest. It should be noted that the square root in the definition of Ar is only used in connection with envelope flows, when it can be interpreted as a velocity ratio. For large Ar values buoyancy forces will dominate. $Ar^{0.5}$ can be defined in (3) as where H is the opening height in question.

$$Ar = \frac{\Delta T_{ie}\, g\, H}{\bar{T}_i\, {v_w}^2} \tag{3}$$

The ventilation parameter, Flow Number F, is a practical dimensionless number to describe wind induced ventilation. Generally where flow is buoyancy dominated F should approach the asymptote defined by F_{th}. When wind dominates $Ar^{0.5}$ tends to zero and F becomes independent of $Ar^{0.5}$. For parallel flows F should be approximately constant at 0.03. F can be defined as:

$$F = \frac{q_{ACH}}{A_{eff} v_w} \tag{4}$$

Plotting these vales for each test allows an interpretation of the influence wind forces have on the buoyancy effect, either assisting or opposing its contributing force.

5 TEST CONDITIONS & RESULTS

5.1 Test conditions

Figure 2 presents polar frequency plots of wind speeds distributed according to wind direction for each test configuration summarised in Table 3 of (O'Sullivan and Kolokotroni. 2014). An analysis of wind data for each test using directional statistics (Mardia. 1972) shows that the mean resultant length of direction vectors, a measure of "concentration" for circular data such as wind direction, were in many instances close to 1.0 with low dispersion of wind orientation during individual tests. This suggests that wind direction was consistent during a given test and the resulting analysis can assume to represent the effects from flow phenomena present for this type of orientation relative to the ventilation opening. We have taken Parallel flow to occur between wind directions of 347.5° – 22.5° & 157.5° – 202.5°. 270° wind direction is normal to the ventilation opening.

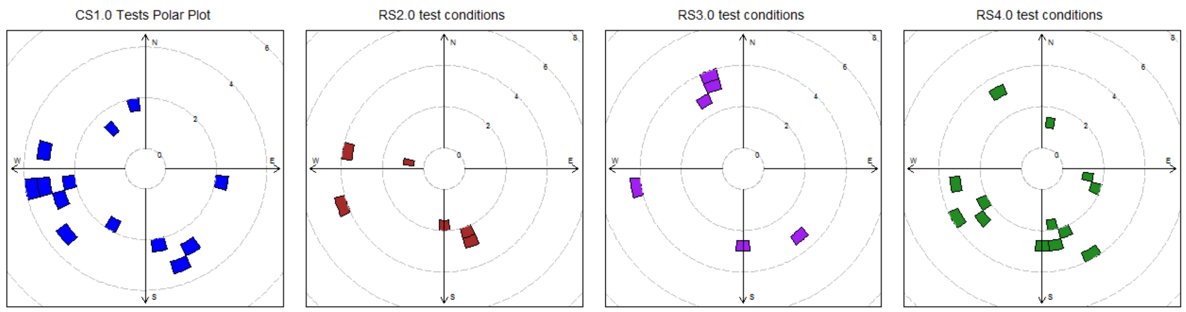

Figure 2: Polar plots for each set of test configuration for different wind speed and wind direction combinations

5.2 Dominant driving forces

Figure 3 presents measured air changes rates as a function of wind direction categorised according to envelope temperature difference and grouped according to test configuration. Figure 4 presents Warren plots for CS.01 & RS.04 and figure 5 presents Warren plots for RS depending on configuration and wind orientation. The purpose of the different plots is to highlight any trends that relate to opening geometry, test environment or driving forces present.

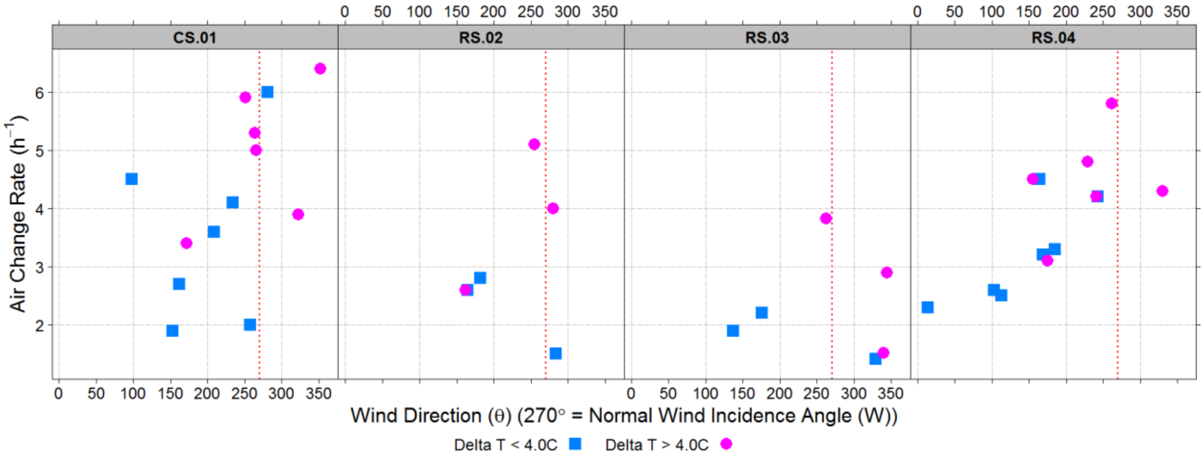

Figure 3: Test Config ventilation rates (h^{-1}) as a function of wind direction grouped according to ΔT_{ie}

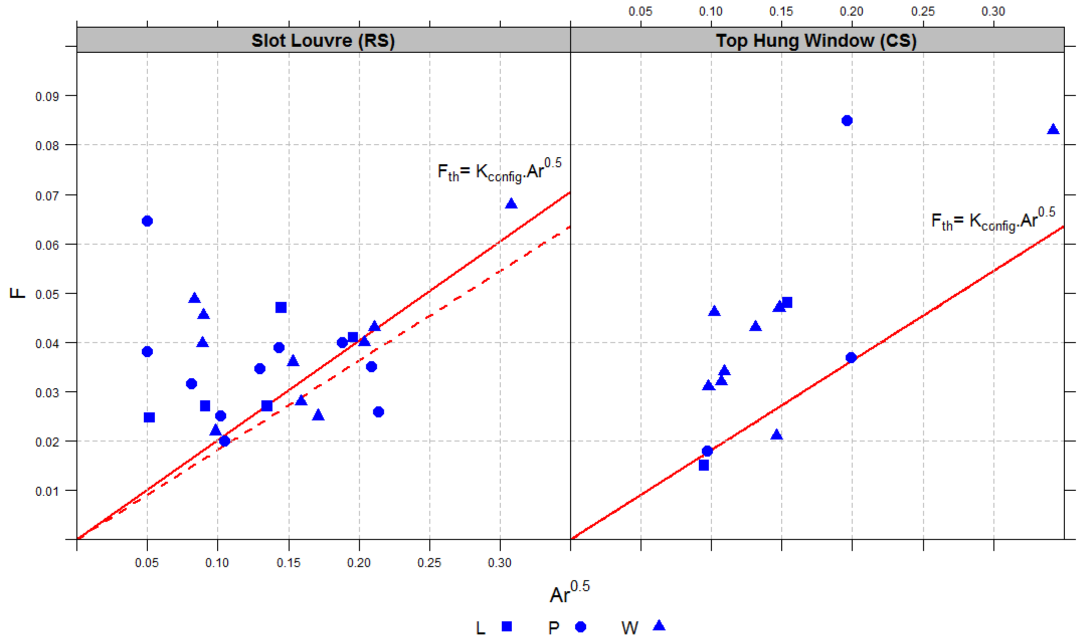

Figure 4 Warren plots for (a) slot louvre system in RS and (b) top hung window in CS. (F_{th} shown in red)

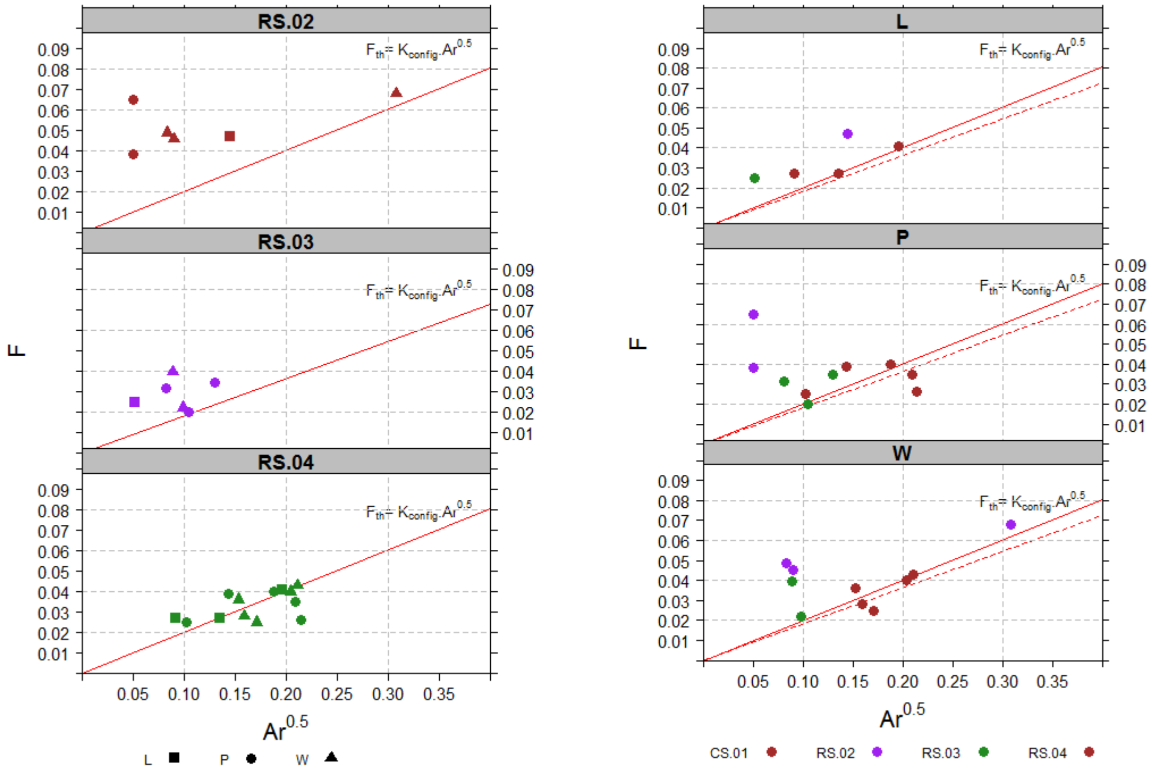

Figure 5 Warren plot categorised according to (a) configuration and (b) wind direction. (F_{th} shown in grey)

5.3 Transient ventilation rates

Single sided ventilation strategies rely on a number of low and high frequency unsteady flow phenomena relating to wind pressure, gustiness and turbulence. Tracer decay rates were measured at a frequency of 1Hz during each test and figure 6 presents ACH values as a function of wind direction, (270° = Normal to surface), grouped according to, σ_c, that is based on the estimate of error in prediction from the regression model fitted to the normalised concentration decay, C_N, to determine the ACH values (O'Sullivan and Kolokotroni. 2014). This is taken as an indicator of the level of unsteadiness present during each test.

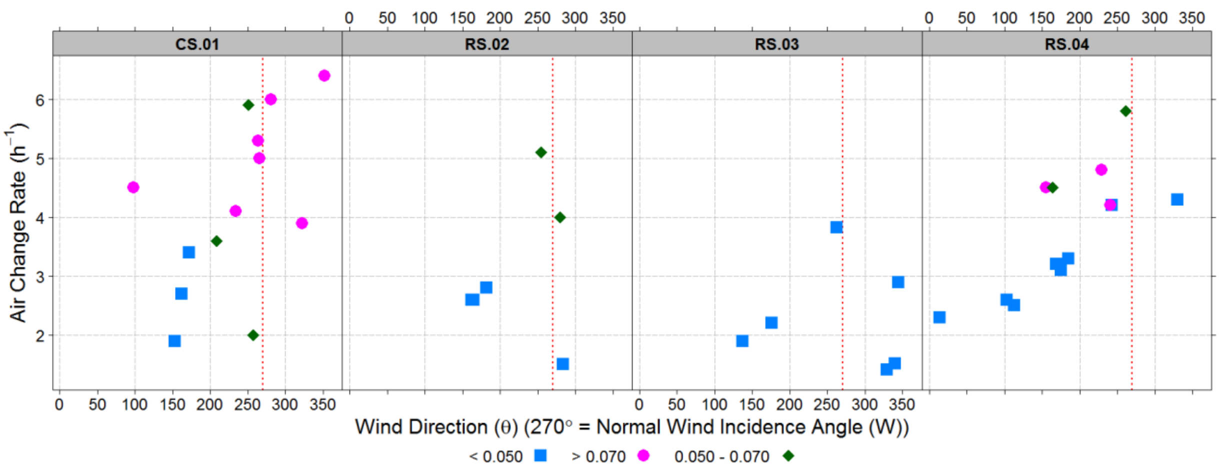

Figure 6: Air Change rate as a function of wind direction grouped according to magnitude of σ_c

6 ANALYSIS & DISCUSSION

6.1 Dominant driving forces

Considering figure 3 in all instances the highest recorded air change rates occurred with ΔT_{ie} greater than 4°C and a windward incidence direction. This occurs in both control and retrofit spaces. Leeward conditions lead to the lowest ventilation rates (although the test population is small for this wind incidence) with parallel incidence directions showing less defined patterns. Low ΔT_{ie} generally resulted in lower ventilation rates for low opening height RS.02 & RS.03 and some CS.01 & RS.04 tests have ACH values higher than 4.0 h^{-1} even at ΔT_{ie} below 4.0°C. It appears that where the wind incidence angle is not approximately normal to the surface then it is more likely to have lower ventilation rates even at relatively high ΔT_{ie} values. This suggests that leeward and parallel flows at the opening are more likely to oppose buoyancy forces. Considering Figure 4(a) & 4(b) we see a comparable spread of F values for both spaces with the retrofit $Ar^{0.5}$ range extending further towards zero ordinate. F seems to display slightly higher dependency on $Ar^{0.5}$ in CS.01. No clear patterns are visible from review of the combined datasets. However, when looking at figure 5(a), when the data in figure 4(a) is split according to RS opening configuration three different patterns emerge. RS.04, ($H_{ope} = 1.60m$), shows a clear pattern of buoyancy dominant ventilation irrespective of the wind incidence angle, which seems to agree with data in figure 3 where the highest RS.04 ventilation rates had high ΔT_{ie} values. Alternatively RS.03 has $H_{ope} = 0.76m$ (H_{int}= 2.43m (above floor level)) and also has a potentially lower C_d value than RS.02. It exhibits increased contributions from wind forces with similar F values but consistently lower $Ar^{0.5}$ values compared to RS.04. It appears that with lower opening height buoyancy forces have less ability to establish resulting in lower $Ar^{0.5}$ values and as a result F values appear more independent of $Ar^{0.5}$ in lower ranges. RS.02 ($H_{ope} = 0.76m$) (($H_{int} = 1.59m$) has a greater internal door opening angle than RS.03. It exhibits the least dependency on buoyancy forces with nearly all tests showing wind dominant F values. The clear variation in response of each opening location presents a situation where for the slot louvre system the contribution from momentum forces is a function of the overall structural opening height and vertical location on the envelope. Considering figure 4(b) leeward tests seem to display a good range of $Ar^{0.5}$ values and a general trend of F values near the asymptote F_{th}. According to (Caciolo et al. 2013) leeward conditions should be counteractive to buoyancy forces. This is not the case here with the slot louvre opening. Only one of the five leeward tests had ΔT_{ie} < 4.0°C. Both Parallel and Windward incidence angles show a pattern of reducing dependency of F on $Ar^{0.5}$ as its value tends to zero. At low $Ar^{0.5}$ F is a function of wind incidence direction. At higher values these incidence angles show a tendency towards the asymptote and the wind direction effects are diminished. These results are in line with (Larsen and Heiselberg, 2008) in showing the interdependence of F on both $Ar^{0.5}$ and wind direction and suggest that at low $Ar^{0.5}$ wind incidence angle becomes important in determining whether or not wind becomes dominant.

6.2 Ventilation rate characteristics

While it is difficult to draw any clear quantitative conclusions regarding high frequency fluctuating phenomena when examining time averaged test data, the concentration fluctuation parameter, σ_c (based on 10 second averages of readings taken at 1Hz), can still give a measureable indication of the overall unsteadiness present in a ventilated space during a tracer decay test. Figure 6 groups ACH data according to σ_c. The causes of this unsteadiness can be due to several factors: pulsation flow, penetration of eddies, and static or molecular diffusion. It is difficult to isolate the specific causes without detailed measurements of these various phenomena and an assessment of overall trends is the most that can be achieved at this point. 10 of the 13 CS.01 window opening tests exhibited unsteadiness at the upper end of all recorded σ_c values and these appeared to happen primarily under windward incidence directions. These tests had averaged wind speeds > 3.0 ms^{-1}, ΔT_{ie} > 5.0°C and appear wind dominant according to the Warren plot analysis. This would suggest that unsteady ventilation rates are more pronounced when wind is normal to the outward opening window. This may be due to the nature of flow impingement with the window obstructing entry resulting in increased turbulence. The highest fluctuation value for parallel flow in CS.01 happened with one of the lowest average test wind speeds ($1.8\ ms^{-1}$) while the two other parallel flow tests showed lower unsteadiness profiles with lower F values suggesting that with parallel flow and an outward opening window fluctuating components of ventilation rate are less pronounced and buoyancy driven flow is able to better establish. This may be due to the fact the opening section of the window does not obstruct parallel flow at the boundary layer of the structural opening. More parallel flow tests are needed before this is conclusive. In the slot louvre system only RS.04 exhibits tests with significant unsteadiness and all these tests occurred at windward incidence angles. Higher fluctuation parameters are associated with higher ventilation rates in RS.04 suggesting the importance of turbulence and wind induced phenomena to single sided ventilation rates. These also occurred at windward incidence directions. For RS.03 & RS.02, irrespective of wind incidence angle fluctuation parameters were always low as were ventilation rates. Warren plot analyses suggest these are generally wind dominant with low $Ar^{0.5}$ but they consistently exhibited low σ_c values appearing counter intuitive. When comparing fluctuation rates for parallel flow in the RS configuration they are generally lower than windward incidence angles. What is apparent from the test data is the opening geometry has a direct influence on the nature of ventilation rate and wind incidence direction also plays an important role with its effect dependant on the opening geometry.

7 CONCLUSIONS

Previous work presented in (O'Sullivan and Kolokotroni, 2014) have highlighted the potential interdependence of F on both $Ar^{0.5}$ and wind direction, particularly at low $Ar^{0.5}$ values. This paper investigated this further and has shown that the magnitude of $Ar^{0.5}$ to be dependent on opening geometry. In physical terms this interdependence highlights the challenges in predicting the correct airflow phenomena driving ventilation for different types of natural ventilation components. An allowance for wind incidence direction, opening height and aspect ratio and opening location in relation to the internal space will affect ventilation rates. If σ_c is taken as an indicator of internal airflow environment for single sided ventilation this suggests the interdependence of opening geometry and wind incidence direction has a large influence on the penetration of wind-generated air exchange mechanisms. Modification of thermophysical properties due to the retrofit have reduced the magnitude of $Ar^{0.5}$ for similar F values suggesting wind driving forces have an increased contribution even though the slot louvre system is perceived as restricting flow. Further tests including measurements directly at the external and internal faces of the opening will increase understanding of the providing a more definitive allocation of the effect of the parameters investigated; such measurements are under progress. Further work will include CFD model of the slot louvre systems and this would allow further analysis of the effect of opening geometry on unsteadiness magnitudes.

8 ACKNOWLEDGEMENTS

The authors wish to thank Dr Peter Warren for his very helpful discussions and advice regarding the use of the Warren plots. The original pilot project works was supported through a grant from the Department of Education and Skills, Ireland. The authors wish to acknowledge the co-work of the pilot project design and research team in the design and development phases of the pilot project

9 REFERENCES

Caciolo, M., Cui, S., Stabat, P., Marchio, D. (2013) "Development of a new correlation for single-sided natural ventilation adapted to leeward conditions," Energy & Buildings, 60, 372–382,

Caciolo, M., Stabat, P., Marchio, D. (2011) "Full scale experimental study of single-sided ventilation : Analysis of stack and wind effects," *Energy & Buildings*, 43(7), 1765–1773,

Chiu, Y.-H., Etheridge, D.W. (2007) "External flow effects on the discharge coefficients of two types of ventilation opening," *Journal of Wind Engineering and Industrial Aerodynamics*, 95(4), 225–252,

Cockroft, J. P., & Robertson, P. (1976), Ventilation of an enclosure through a single opening, *Building and Environment,* 11(1), 29-35

Crommelin, R. D., & Vrins, E. M. H. (1988), Ventilation through a single opening in a scale model, *Air Infiltration Review*, 9(3), 11-15

Dascalaki, E., Santamouris, M., Argiriou, A., Helmis, C., Asimakopoulos, D.N., Papadopoulos, K., Soilemes, A. (1996) "On the combination of air velocity and flow measurements in single sided natural ventilation configurations," *Energy and Buildings*, 24(2), 155–165

Dascalaki, E., Santamouris, M., Argiriou, A., Helmis, C., Asimakopoulos, D. N., Papadopoulos, K., & Soilemes, A. (1995). Predicting single-sided natural ventilation rates in buildings, *Solar Energy*, 55(5), 327-341

de Gids, W., & Phaff, H. (1982). Ventilation rates and energy consumption due to open windows: a brief overview of research in the Netherlands. *Air infiltration review*, 4(1), 4-5

Etheridge, D., 2011. *Natural Ventilation of Buildings: Theory, Measurement and Design*, Wiley-Blackwell.

Grabe, J. Von (2013) "Flow resistance for different types of windows in the case of buoyancy ventilation," *Energy and Buildings*, 65, 516–522,

Von Grabe, J., Svoboda, P., Bäumler, A. (2014) "Window ventilation efficiency in the case of buoyancy ventilation," *Energy and Buildings*, 72, 203–211

Heiselberg, P., Svidt, K., Nielsen, P. (2001) "Characteristics of airflow from open windows," *Building and Environment*, 36, 859–869

Irving, S., Etheridge, D., Ford, B. (2005) *Natural Ventilation in Non-Domestic Buildings CIBSE AM10*, The Chartered Institution of Building Services Engineers, CIBSE.

Karava, P., Stathopoulos, T., Athienitis, A. (2004) "Wind driven flow through openings–a review of discharge coefficients," *International Journal of …*, 3(3)

Larsen, T.S., Heiselberg, P. (2008) "Single-sided natural ventilation driven by wind pressure and temperature difference," *Energy and Buildings*, 40(6), 1031–1040

Mardia, K. V. (1972). Statistics of directional data, Academic Press

O'Sullivan, P., Kolokotroni, M. (2014) "Time-averaged single sided ventilation rates and thermal environment in cooling mode for a low energy retrofit envelope system." *International Journal of Ventilation* (In Press)

Pinnock, D. (2000) *An Investigation into the Influence of Wind in Single-Sided Natural Ventilation,* available: https://dspace.lboro.ac.uk/xmlui/handle/2134/7465

Sharples, S., Chilengwe, N. (2006) "Performance of ventilator components for natural ventilation applications," *Building and Environment*, 41(12), 1821–1830,

Van der Maas, J. (1992). *Air Flow Through Large Openings in Buildings (Subtask 2): IEA Annex 20–Air Flow Patterns Within Buildings*, LESO-PB, EPEL, CH-1015. International Energy Agency, Lausanne, Switzerland

Wang, H., Chen, Q. (2012) "A new empirical model for predicting single-sided , wind-driven natural ventilation in buildings," *Energy & Buildings*, 54, 386–394,

Warren, P., Parkins, L. (1985) "Single-sided ventilation through open windows," *ASHRAE SP49*, (1),